IEEE Photonics Journal
An IEEE Photonics Society Publication

Mechanical Scan-Free Confocal Microscope by a Broadband Source and Two Balanced Wavelength-to-Space Transformations

Volume 7, Number 1, February 2015

Hsien-Yi Wang
Bor-Shyh Lin, Member, IEEE
Chien-Ya Lou
Ming-Che Chan

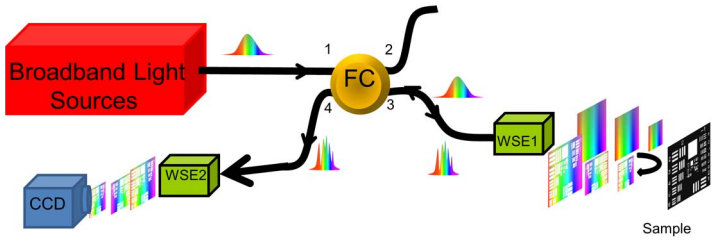

DOI: 10.1109/JPHOT.2015.2390617
1943-0655 © 2015 IEEE

Mechanical Scan-Free Confocal Microscope by a Broadband Source and Two Balanced Wavelength-to-Space Transformations

Hsien-Yi Wang,[1] Bor-Shyh Lin,[2] *Member, IEEE*, Chien-Ya Lou,[2] and Ming-Che Chan[2]

[1]Department of Nephrology, Chi-Mei Medical Center, Tainan 710, Taiwan
[2] College of Photonics, National Chiao Tung University, Tainan 711, Taiwan

DOI: 10.1109/JPHOT.2015.2390617

Manuscript received December 2, 2014; revised January 7, 2015; accepted January 8, 2015. Date of current version January 27, 2015. This work was supported in part by the National Science Council of Taiwan under Grant NSC 100-2221-E-009-092-MY3 and Grant NSC 103-2221-E-009-076 and in part by the Chi-Mei Medical Center, Tainan, under Grant CMCT10305, Grant CMFHR 10361, and Grant CMFHR 10211. Corresponding author: M.-C. Chan (e-mail: mcchan@nctu.edu.tw).

Abstract: A new approach for performing confocal microscopy without no mechanical scanners was reported by a broadband light source, two similar 2-D wavelength-dispersive optical elements, and an uncooled charge-coupled device (CCD). In the new approach, 2-D sample structures were simultaneously and instantly mapped into the CCD by performing two balanced wavelength-to-space transformations and one space-to-wavelength transformation. Compared with a traditional mechanical-scanner-based confocal microscope, no mechanical scanners or additional post dataprocessing were required in this new approach. The sectioned images are directly shown in the CCD. The demonstrated balanced wavelength-encoded confocal microscope has a simple configuration and shows great potential for high imaging speed. It has the advantage of miniaturized packaging and other applications outside of the laboratory as well.

Index Terms: Confocal microscope, broadband source, diffractive optics, wavelength encoded.

1. Introduction

Since the invention of confocal microscopy, it has become an important diagnosis tool widely used in the biological, medical, industrial, semiconductor, and physical fields due to its capability in noninvasively imaging sectioned microstructures inside thick specimens with a high contrast and a micro-meter resolution [1], [2]. Currently, besides the basic research requiring maximum performance inside the laboratory, the major focus of research on confocal microscopy is to develop higher speed, miniaturized, and simpler imaging instruments [3]. This is due to the fact that motion artifacts can be avoided with a high speed confocal microscope. Moreover, a simple and miniaturized confocal microscope can be easily incorporated into an endoscope or a catheter or even into charge-coupled device (CCD) cameras inside smart-phones, which is utilized to image microscope structures inside a hollow cavity or outside of the laboratory environments.

However, in a traditional laser scanning confocal microscope, bulky mechanical beam scanners are usually needed so that the excitation laser beams are sequentially focused on the samples point to point by scanners and an objective. The reflected light, encoded by 2-D sample

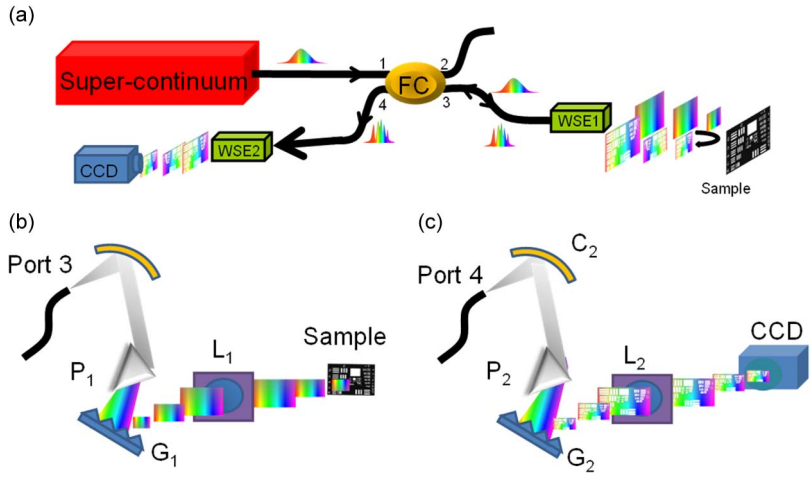

Fig. 1. (a) Schematic representation of the balanced 2-D mechanical scan-free confocal microscope. FC: fiber coupler; WSE_1 and WSE_2: Wavelength-space-encoder. CCD: Charge-coupled devices. (b) Schematic of wave-to-space transformations in the sample side. C1: Collimator. P1: Prism. G_1: Grating. L_1: Focusing Lens. (c) The schematics in the CCD side. C_2: Collimator. P_2: Prism. G_2: Grating. L_2: Focusing Lens. Note the schematic on the CCD side is symmetrical to that on the sample side.

structures in the time domain, was detected and then decoded into images by computers. These mechanical scanners introduce fluctuations or noise during the process of image acquisition. Furthermore, miniaturizing mechanical scanners, such as galvanometers, resonant mirrors, and spinning polygons, remain a challenge to the development of hand-held compact microscopes and endoscopes for imaging inside hollow tissue cavities [4].

To date, for replacing one or two bulky mechanical scanners inside confocal microscopes, various wavelength-to-space disperser(s) was utilized in confocal microscope [4]–[10]. In the wavelength-to-space disperser(s), different wavelength components of the excitation source's emission spectrum are focused and mapped to different positions within the sample by various diffractive or dispersive optical elements, such as gratings [4]–[6], virtually imaged phase arrays (VIPAs) [7], [8], prisms [9], or Fresnel lens [10], [11]. The reflected optical spectrum from the specimen is then encoded for the sample structure. The encoded spectrum is then passed through the confocal pinhole and decoded at the detection end by different optical systems, such as the heterodyne Fourier-transform spectroscopy [4], the optical spectrometry [5], [7], [10], [11], or a high-speed detection system [6], [8]. In these decoding systems, additional post data-processing hardware and software procedures are needed to deduce the 2-D or 3-D sample image according to the sample-encoded spectrum, which increases the system's complexity and slows down the imaging speed.

In this paper, we proposed and demonstrated a new approach to mechanical scan-free confocal microscope with a super-continuum source, two balanced 1-D or 2-D wavelength-to-space dispersers and an un-cooled CCD. The Core components of the proposed wavelength-encoded confocal microscope are two similar 1-D or 2-D wavelength-to-space dispersers which symmetrically transform the sectioned sample structures onto the CCD chip instantaneously, without requiring mechanical scanners on the sample side or additional post data-processing process for image recovery. The demonstrated balanced 2-D wavelength-encoded confocal microscope is simple in configuration, and has the advantages of high imaging speed and miniaturized packaging, which could thus make it ideal for many biological and clinical applications.

2. Experimental Details

Fig. 1(a) shows a schematic diagram of the 2-D mechanical scan-free confocal microscope. A broadband super-continuum source was used as the excitation light source, which output

bandwidth spanned from 450–2400 nm. The excitation source was connected to a 50/50 directional fiber coupler (FC-632-50B-APC, Thorlabs). One terminal of the 50/50 coupler (Port 2) was angle-cleaved. Index-matching oil was used to eliminate reflection from the fiber–air interface, which could produce a strong noise background in the confocal microscope. The measured intensity of reflected light was at least 60 dB lower than that of transmitted light in Port 2 throughout the experiment. At the other output terminal (Port 3), as can be seen in Fig. 1(b), the input beam was collimated by a reflective parabolic collimator (RC08APC-P01, Thorlabs). The collimated beam, with an 8 mm beam size, was then dispersed by a 2-D wavelength-to-space disperser, which consists of a prism in the vertical direction (y-axis) and a grating in the horizontal direction (x-axis).

Fig. 1(b) shows that the optical spectrum was converted to a spatial–spectral pattern in the wavelength-to-space disperser. First, the prism with a 60 degree apex angle dispersed the broadband excitation light into a 1-D spatial–spectral pattern. The 1-D vertical spatial–spectral pattern was then transformed into a 2-D spatial–spectral pattern by a grating with a 1200 line/mm groove density. According to the prism equation and grating equation [12], the calculated angular dispersions of the prism and grating in this experiment were 0.00216 degrees/nm and 0.0834 degrees/nm, respectively. The formed 2-D spatial–spectral pattern was focused onto the sample by an achromatic doublet (AC-027-019-B-ML, Thorlabs) with a 1.9 cm focal length. The 2-D wavelength-to-space dispersers and focusing lens formed one-to-one spatial mapping between the excitation wavelength and 2-D spatial coordinates in the focal plane of L_1. The reflected 2-D spatial–spectral pattern from the sample, encoded by the sample structure, was converted into the same single point light source by the same wavelength-space mapping optical elements, as shown in Fig. 1(a). The core of the collection fiber at Port 3 also acted as a confocal pinhole rejecting the out-of-focus reflected light. The reflected light (in the wavelength domain) from Port 3 was directed to Port 4 by the same 50/50 coupler. As shown in Fig. 1(c), the 2-D spatial–spectral pattern, encoded by the specimen structure, was dispersed by a similar 2-D wavelength-to-space disperser [see Fig. 1(b)], and focused onto an un-cooled Silicon CCD (PL-B959, EO Edmunds) offering a frame rate up to 15 Hz.

3. Experimental Results

In order to quantitatively characterize the limitation of available bandwidth, produced from the fiber coupler, focusing lens, wavelength-dispersers and CCD, we first performed 1-D wavelength encoded confocal microscopy. In the 1-D microscope, the 2-D wavelength-to-space disperser, shown in Fig. 1(b) and (c), was replaced by a 1-D wavelength-to-space disperser which is composed of single prism only. The system performance of the proposed mechanical scan-free confocal microscope was characterized using a USAF-1951 resolution target as a test sample. Behind the resolution target is a miniaturized digital microscope (UPG-620, UPMOST) which was used to monitor the location of the illuminated 1-D spatial–spectral pattern. Fig. 2(a) shows the typical spectrum of the super-continuum light after Port 3. The spectrum of the super-continuum cannot be fully used here due to limited bandwidth of the 50/50 fiber coupler and the CCD. A USAF-1951 resolution target was used as the first test sample.

Fig. 3(a) shows the unprocessed image of a group of seven elements on the test target and the inset shows a magnified image of the area inside the dashed box in Fig. 3(a). For Elements 2 to 6 in group 7, clearly observed in the inset, show that the resolution was better than 2.28 μm which is the smallest pitch width in the resolution chart. Fig. 3(b) shows the schematic of all elements in the Group 6 and 7 of the USAF-1951 resolution chart for comparing the imaging of the resolution chart. On the other hand, the reference microscope image, indicating the locations of 1-D corrugated spectral–spatial pattern, is shown in Fig. 3(c). It was acquired from the back side of the resolution chart by the compact USB microscope. From Fig. 3(c), the 1-D spatial–spectral pattern was illuminated on the elements 2 to element 6 of Group 7. The position of illumination pattern is also marked as the red-dashed line in Fig. 3(b). By comparing Fig. 3(b) and the inset of Fig. 3(a), the elements 6 in group 7, with a 2.28 micron pitch size, can be resolved in the inset of

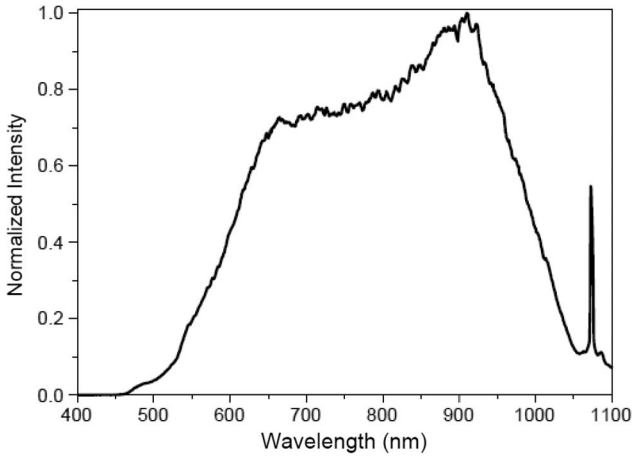

Fig. 2. (a) Spectrum measured at Port 2 of the balanced 2-D wavelength-encoded confocal microscope. (b) 1-D confocal images of the resolution chart, where element 6 of group 7 can be resolved. Inset: Enlarged image of area inside the dashed box. The prism pair (P1 and P2) gives a single vertical wavelength-encoded axis.

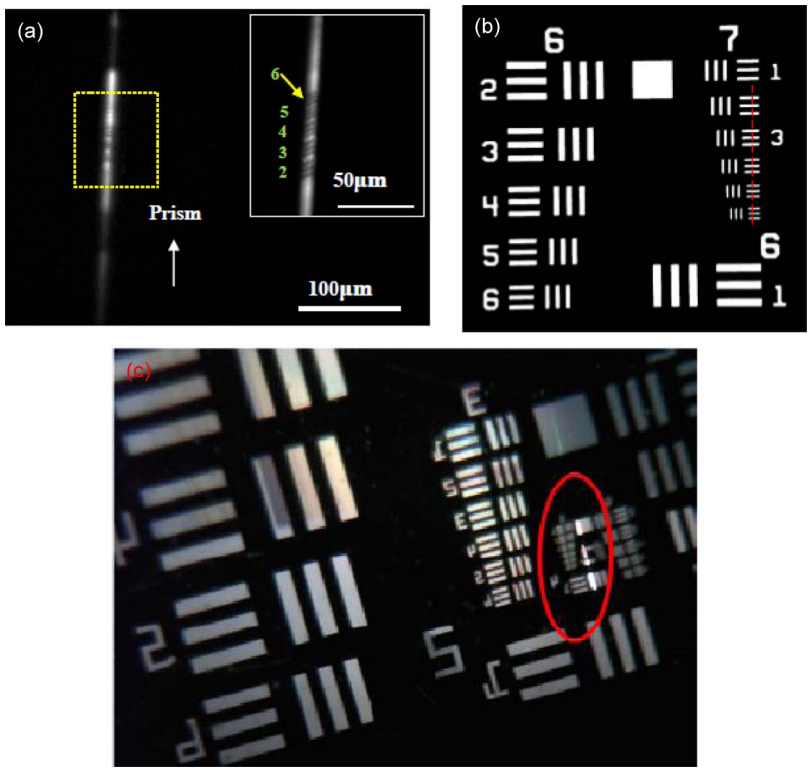

Fig. 3. (a) One-dimensional confocal images of the resolution chart, where element 6 of group 7 can be resolved. (Inset) Enlarged image of area inside the dashed box. The prism pair (P_1 and P_2) gives a single vertical wavelength-encoded axis. The number inserted in the inset of (a) indicates the number of elements. (b) Schematic of the Group 6 and 7 elements of the USAF-1951 resolution chart. The dashed red-line indicates the position of the 1-D illuminated pattern. (c) Reference microscope image of the 1-D illuminated pattern, enclosed within the red circle, from the back side of the resolution chart.

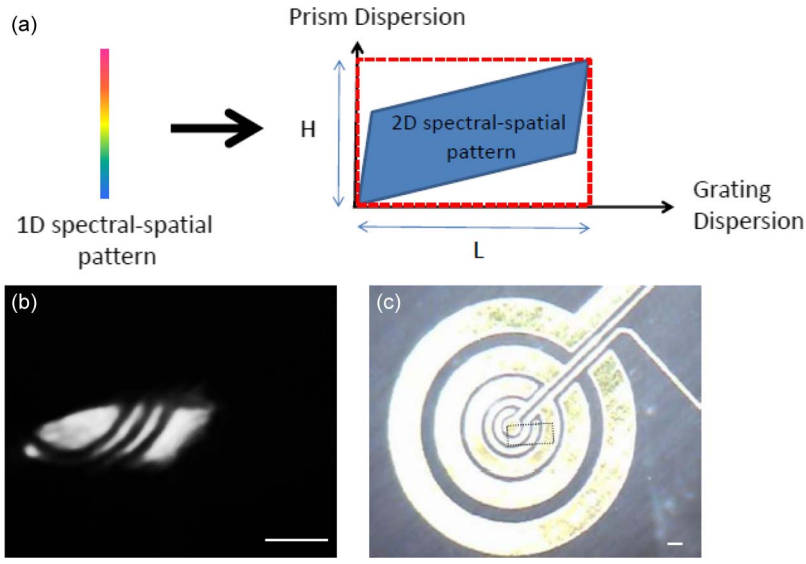

Fig. 4. (a) Schematic of the 1-D (colored bar) and 2-D spectral–spatial illumination pattern. The dashed red-box indicates the theoretical image size. (b) Two-dimensional wavelength-encoded confocal image of an inter-digital electrode. Note that prism pair (P_1 and P_2) gives the vertical wavelength-encoded axis and grating pair (G_1 and G_2) gives the horizontal wavelength-encoded axis. (c) Bright-field microscopic image of the inter-digital electrode. The image corresponding to the area in the dashed box is shown in (a). (c) Image of a tissue paper sample. Scale bars for Fig. 3(b) and (c) 100 μm.

Fig. 3(a). The marked element numbers are also added into the inset of Fig. 3(a) to indicate the element number of Group 7.

On the other hand, Fig. 3(a) shows the 1-D corrugated pattern with an observed length of $\sim$314 μm.

Assuming a 1-D wavelength-to-space disperser with angular dispersion $\partial\theta/\partial\lambda$, a lens with a focal length f and the field of view (FOV) can be defined by the following equation:

$$\text{FOV} = \left(\frac{\partial\theta}{\partial\lambda}\right) \cdot \Delta\lambda \cdot f. \tag{1}$$

In (1), the angular dispersion should be calculated in radians. Based on the measured FOV and the theoretical angular dispersion and focal length, we can calculate that the available bandwidth was about 438.4 nm. Compared with the measured spectrum at Port 3, shown in Fig. 2, for this new confocal microscope, we can estimate that the upper limit of the available wavelength was located in the 500–600 nm wavelength regimes and the lower limit of the available wavelength in the 1000–1100 nm regimes.

From the 1-D measurement, the available bandwidth and resolution were determined. One can add another 1-D mechanical scanner, such as a stepping motor or Galvono mirror, to perform 2-D confocal images. In this work, we perform 2-D confocal images by the proposed 2-D mechanical scan-free confocal microscope.

Fig. 4(a) shows the schematic of the 2-D spectral–spatial pattern which is similar to a parallelogram. The super-continuum light was dispersed into a 1-D spatial–spectral pattern, as shown in the color bar in Fig. 4(a), by the prism with a 60 degree apex angle, and the 1-D spatial–spectral pattern is then dispersed into the 2-D pattern by the grating. The theoretical image shape is shown in the red-dashed box of Fig. 4(a). The size can be easily calculated individually according to the prism equation and grating equation. From Fig. 2, assuming the upper and lower limit of the available wavelength were 500 nm and 1000 nm, respectively. According to the prism equation with 60 degree apex angle, the refraction angle difference between the 500 nm and 1000 nm beam is 1.08 degrees. With a lens with 19 mm focal length, the length of the prism-dispersed beam was 358 μm (H). On the other hand, the refraction angle difference between the

500 nm and 1000 nm beam was 41.7 degrees. The calculated theoretical length of grating-dispersed beam was 13.82 cm (L). However, in the experiment, instead of a rectangular patter, the 2-D illumination pattern is like a parallelogram. The 1-D spatial–spectral pattern which is divided into many sub-sections with a smaller bandwidth. Each sub-section was individually dispersed by a grating with a 1200 lines/mm groove density to form a 2-D illumination pattern. However, the ratio between the base and height of the 2-D parallelogram pattern on the sample is strongly dependent on the angular dispersion ratio of prism and grating, the bandwidth of each sub-section in the 1-D spectral–spatial pattern, and highly wavelength-dependent diffraction efficiencies of gratings.

Based on the configuration described in Fig. 1(a), the 2-D mechanical scan-free confocal imaging is performed. An inter-digital electrode was utilized used as a test sample to obtain the experimental image size of this proposed 2-D mechanical scan-free confocal microscope. Fig. 3(b) shows the confocal image of the inter-digital electrode. Sectioned images of metal electrodes can be directly obtained from CCD, as described above. By moving the sample, the measured image size was 348 μm by 143 μm. The image size can be also be double confirmed by the corresponding bright field microscopic image of the inter-digital electrode is shown in Fig. 3(c). In the 2-D confocal measurement experiment, the typical integration time of the CCD was below 30 ms on the samples exposed to under an illumination with power of 100 μW. In this experiment, the images in Fig. 3(b) (confocal image) and Fig. 3(c) (reference microscope image) are a little distorted because of the un-perfectly matched optical arrangements between the sample arm (Port 3) and the CCD arm (Port 4). The perfectly matched optical arrangements, including the identical orientations and relative positions between all optical elements in Port 3 and Port 4, can be achieved by Micro-Opto-Electro-Mechanical-Systems (MOEMS) technology, where all optical elements are fabricated at the same time with fixed distances.

The preliminary results, shown in Fig. 3 (b), demonstrate the real-time capability of using the proposed 2-D mechanical scan-free confocal microscope method for the imaging of industrial or biological samples. Moreover, the mechanical scan-free confocal microscopes also have the potential for integration since all the elements, including the collimator, prism, and grating in the sample arm (Port 3) and CCD arm (Port 4) could be further miniaturized using graded-index collimators, micro-prisms and holographic gratings, collectively. The core of the collimation fiber at Port 3 rejects the out-of-focus reflected light so that the confocal pinhole could be removed thereby further simplifying the system. The fiber-based confocal system also provides flexibility and easy maintenance. Thus, a maximum CCD rate was 15 frames per second. By incorporating two balanced 2-D wavelength-to-space dispersers, the sectioned structures of the sample were simultaneously mapped onto the CCD without mechanical scanners on the sample side, nor the addition of a post decoding procedure along the 2-D wavelength encoded axis (x and y) for image recovery.

4. Discussions

A frame rate of up to 15 Hz, limited by the available CCD frame rate, was achieved with the demonstrated 2-D mechanical scan-free confocal microscope. Since there was no post-data processing procedure, using a higher-speed CCD is a viable way to increase the frame rate in the proposed mechanical-scan free confocal microscope. Currently, high-speed CCDs with a frame rate of several MHz have been developed [13] and integrating this kind of CCD in our proposed system is helpful to increase the frame rate. For the sample viability, the sample cannot be illuminated with high-power light. Therefore, on the other hand, another limitation to obtain the higher imaging speed is the trade of the sensitivity and frame rate [7], [8] under limited illumination power for sample viability. This limitation can be resolved by inserting a broadband amplifier in Port 4 where the image amplification in the optical domain might be a solution [7], [8].

For the imaging area, the image size (Field of View) can be increased, as shown in (1), by increasing the focal lens of L_1, the available working bandwidth, and the angular dispersion of the 2-D wavelength-to-space disperser. Increasing the focal lens of L_1 will degrade the image

resolution. The available working bandwidth is limited both by the bandwidth of the light source and the wavelength response of the optical elements used in the proposed 2-D mechanical scan-free confocal microscope comprising the 50/50 fiber output coupler, prism, grating and CCD. To increase the available working bandwidth, the fiber coupler can be replaced with a traditional beam splitter with a wider bandwidth or an ultra-broadband fiber coupler [17] with a more than 1000 nm bandwidth. On the other hand, the working bandwidth can be extended by connecting another IR CCD in parallel the silicon-based CCD because the Silicon-CCD's operational wavelength is below 1100 nm. Finally, the angular dispersion can be increased by incorporating highly-wavelength-dispersed optical elements, such as VIPA [7], [8] or super-prisms [14]–[16].

The factors limiting the frame rate and image size can be improved by using the technology already available today. This report represents a step toward the production of a mechanical-scan-free miniaturized confocal microscope with a high frame rate and simple configuration. Several improved versions of our system are currently being developed and will be applied to in-vivo studies in the near future.

In this experiment, only sectioned images near the surface was shown because of the poor signal to noise ratio (SNR) of the 2-D wavelength-encoded confocal system, where all the optical power was simultaneously illuminated on the entire focal plane of sample. The illumination power in each pixel was limited. In this preliminary experiment, the SNR was limited by the average power of the light source and the loss from the diffraction gratings and prisms due to the fact the signal intensity is proportional to the cubic of grating transmission efficiency (twice in Port 3 and once in Port 4). For future confocal in-depth imaging, we require a higher system SNR system which can be implemented by increasing the power of the source and decrease the insertion loss of each optical element in the proposed microscope.

5. Conclusion

In conclusion, a new approach to mechanical scan-free confocal microscope is proposed and demonstrated using a super-continuum source, two balanced 2-D wavelength-to-space dispersers and an un-cooled CCD. With two similar 2-D wavelength-to-space dispersers, sectioned sample structures are symmetrically transferred onto the CCD instantaneously, without requiring any mechanical scanners on the sample side or additional post data-processing process for image recovery. The demonstrated mechanical scan-free confocal microscope, simple in configuration, shows the capability of high imaging speed and miniaturized packaging, making it ideal for many industrial, biological, and clinical applications.

Acknowledgement

The authors are indebted to Prof. Y.-C. Lai of National Chiao Tung University and Prof. C.-K. Sun of National Taiwan University for academic discussions.

References

[1] M. Rajadhyaksha, M. Grossman, D. Esterowitz, and R. H. Webb, “In-vivo confocal scanning laser microscopy of human skin-melanin provides strong contrast,” *J. Invest. Dermatol.*, vol. 104, no. 6, pp. 946–952, Jun. 1995.
[2] R. H. Webb, “Confocal optical microscopy,” *Rep. Prog. Phys.*, vol. 59, pp. 427–471, Mar. 1996.
[3] K. Sokolov *et al.*, “Endoscopic microscopy,” *Dis. Markers*, vol. 18, no. 5/6, pp. 269–291, May/Jun. 2002.
[4] G. J. Tearney, R. H. Webb, and B. E. Bouma, “Spectrally encoded confocal microscopy,” *Opt. Lett.*, vol. 23, no. 15, pp. 1152–1154, Aug. 1998.
[5] L. Golan, D. Yeheskely-Hayon, L. Minai, E. J. Dann, and D. Yelin, “Noninvasive imaging of flowing blood cells using label-free spectrally encoded flow cytometry,” *Biomed. Opt. Exp.*, vol. 3, no. 6, pp. 1455–1464, Jun. 2012.
[6] C. Boudoux *et al.*, “Rapid wavelength-swept spectrally encoded confocal microscopy,” *Opt. Exp.*, vol. 13, no. 20, pp. 8214–8221, Oct. 2005.
[7] K. K. Tsia, K. Goda, D. Capewell, and B. Jalali, “Simultaneous mechanical-scan-free confocal microscopy and laser microsurgery,” *Opt. Lett.*, vol. 34, no. 14, pp. 2099–2101, Jul. 2009.
[8] K. Goda, K. K. Tsia, and B. Jalali, “Serial time-encoded amplified imaging for real-time observation of fast dynamic phenomena,” *Nature*, vol. 458, pp. 1145–1149, Apr. 2009.

[9] H. Makhlouf, A. F. Gmitro, A. A. Tanbakuchi, J. A. fUdovich, and A. R. Rouse, "Multispectral confocal microendoscope for in vivo and in situ imaging," *J. Biomed. Opt.*, vol. 13, no. 4, Jul./Aug. 2008, Art. ID. 044016.
[10] K. B. Shi, P. Li, S. Z. Yin, and Z. W. Liu, "Chromatic confocal microscopy using supercontinuum light," *Opt. Exp.*, vol. 12, no. 10, pp. 2096–2101, May 2004.
[11] D. Duque and J. Garzon, "Effects of both diffractive element and fiber optic based detector in a chromatic confocal system," *Opt. Laser Technol.*, vol. 50, pp. 182–189, Sep. 2013.
[12] E. Hecht, *Optics*, 4th ed. San Francisco, CA, USA: Addison Wesley, 2002.
[13] T. Arai *et al.*, "A 300-kpixel ultrahigh-speed charge-coupled device with a dynamic range of 48.6 dB at 1 million frames per second," *IEEE Trans. Electron Devices*, vol. 59, no. 4, pp. 1107–1113, Apr. 2012.
[14] L. J. Wu, M. Mazilu, and T. F. Krauss, "Beam steering in planar-photonic crystals: From superprism to supercollimator," *J. Lightw. Technol.*, vol. 21, no. 2, pp. 561–566, Feb. 2003.
[15] J. J. Baumberg *et al.*, "Visible-wavelength super-refraction in photonic crystal superprisms," *Appl. Phys. Lett.*, vol. 85, no. 3, pp. 354–356, Jul. 2004.
[16] A. S. Jugessur *et al.*, "Compact and integrated 2-D photonic crystal super-prism filter-device for wavelength demultiplexing applications," *Opt. Exp.*, vol. 14, no. 4, pp. 1632–1642, Feb. 2006.
[17] Y. Jung, G. Brambilla, and D. J. Richardson, "Optical microfiber coupler for broadband single-mode operation," *Opt. Exp.*, vol. 17, no. 7, pp. 5273–5278, Apr. 2009.